

Field measurements of natural periods of vibration and structural damping of wind-excited tall residential buildings

S. Campbell[†], K.C.S. Kwok, P.A. Hitchcock, K.T. Tse and H.Y. Leung

CLP Power Wind/Wave Tunnel Facility, The Hong Kong University of Science and Technology, Hong Kong S.A.R., P.R.China

(Received June 22, 2006, Accepted August 11, 2007)

Abstract. Field measurements of the wind-induced response of two residential reinforced concrete buildings, among the tallest in the world, have been performed during two typhoons. Natural periods and damping values have been determined and compared with other field measurements and empirical predictors. Suitable and common empirical predictors of natural period and structural damping have been obtained that describe the trend of tall, reinforced concrete buildings whose structural vibrations have been measured in the collection of studies in Hong Kong compiled by the authors. This data is especially important as the amount of information known about the dynamic parameters of buildings of these heights is limited. Effects of the variation of the natural period and damping values on the alongwind response of a tall building for serviceability-level wind conditions have been profiled using the gust response factor approach. When using this approach on these two buildings, the often overestimated natural periods and structural damping values suggested by empirical predictors tended to offset each other. Gust response factors calculated using the natural periods and structural damping values measured in the field were smaller than if calculated using design-stage values.

Keywords: residential; tall buildings; typhoons; full-scale measurement; dynamic characteristics.

1. Introduction

Hong Kong is currently ranked ninth in the world in terms of cost of living, which is caused by the inextricable link to high land prices (Mercer 2006). These high land prices in turn cause high costs in both purchase and rental floor areas. Because these land prices are higher, it is not surprising that the heights of buildings, both commercial and residential, grow increasingly taller to meet demands. The majority of tall residential buildings in Hong Kong are made of reinforced concrete (RC) shear walls owing to its low cost and ability to compartmentalize each floor. It is the understanding of how these taller residential buildings respond to typhoon loading that is the catalyst for the research described in this paper.

Two tall residential buildings in Hong Kong, of planform and construction that are typical in the region, are the subjects of a field measurement program aimed at identifying their wind-induced

[†] Corresponding Author, E-mail: soupy@ust.hk

dynamic response and dynamic characteristics. Two typhoons of approximately 1 year return periods provided excitation with which to measure accelerations of these buildings.

These field measurements along with others performed in the region are compared with common natural period and damping predictors. The limited data of dynamic parameters of buildings of these heights makes this comparison particularly important. Values of natural period and damping may vary widely from the design stage to the actual structure. The effects of this variation are considered in terms of serviceability for the alongwind response of a building, determined through the use of the gust response factor (GRF) approach.

2. Monitoring program

The two subject buildings, designated as buildings C and E in Fig. 1, are part of a residential estate in Kowloon that has a relatively open exposure to winds approaching from the south-west and north-west quadrants, i.e., ranging from approximately 240° to 300° from north, inclusive. For the remaining directions, the surrounding terrain is typical of urban areas in Hong Kong. It is also apparent from Fig. 1 that, depending on wind direction, the adjacent buildings within the estate will also affect the exposure of the two subject buildings.

Buildings C and E are structurally similar, although with different heights of approximately 218 m and 212 m respectively, both being of RC shear wall construction and sharing a common podium along with buildings A, B and D. Three storeys above the podium, lateral forces in each building are resisted by perimeter columns and a central lift core. Those columns support a transfer plate which supports the tower superstructure and allows for a large atrium to be located at the entrance. Above the transfer plate, lateral resistance is shared through a combination of the central lift core and shear walls.

Structural vibrations were measured using two orthogonally-mounted accelerometers in both instrumented buildings, located at the roof level above the highest occupied floor of each structure and inside the core of the structure. The reference axes of the accelerometers, denoted as X and Y in Fig. 1, were aligned with the core walls which, in turn, are aligned approximately 112° and 22° clockwise from North, respectively.

A signal conditioner was used to convert the raw current output from each accelerometer to a DC voltage signal. Data records of 10-minute duration were sampled continuously at 20 Hz using a 16-bit A/D converter and stored on a dedicated PC after signal amplification and the application of a 5 Hz low-pass filter.

Onsite restrictions prevented the installation of an anemometer on either building. Wind records

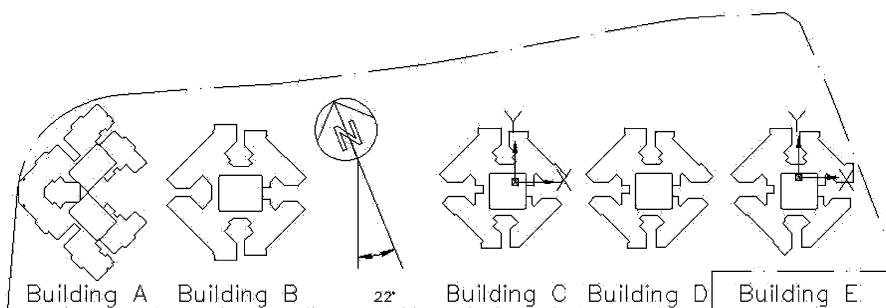


Fig. 1 Field measurement setup for building C and building E

were therefore obtained from an anemometer located on Stonecutters Island, a small island marking the entrance to Hong Kong's shipping container terminals, that is located to the west of the Kowloon Peninsula and approximately 3 km to the northwest of the subject structures. The propeller anemometer is supported on a mast 50 m above ground with near-field topography consisting mostly of water to the southwest, stacked shipping containers to the north, and a 65 m tall hill about 500 m to the east. The measured wind characteristics are considered to generally reflect the overall wind characteristics affecting buildings C and E.

3. Typhoon events

Field measurements of the wind-induced response of the two buildings were conducted during typhoons Imbudo and Dujuan, which affected Hong Kong in 2003. Those typhoons are described in detail in Campbell, *et al.* (2005) and their main features are summarized below.

During typhoon Imbudo the Hong Kong Observatory (HKO) measured the lowest instantaneous mean sea-level pressure of 997.5 hPa at their headquarters on July 24, 2003. The maximum 10-minute mean wind speed was 17.0 m/s and the maximum 3-second gust wind speed was 27.3 m/s, which were both measured on July 23 at Stonecutters Island. The dominant wind direction of typhoon Imbudo tended to be between 50° and 120° from July 23 to 25. This is consistent with the eye of typhoon Imbudo passing to the south of Hong Kong.

While the anemometer at Stonecutters Island better represents the wind field near buildings C and E, it has not been operating for a sufficiently long period for its data to be used alone for a detailed statistical analysis of wind speed and return period. Therefore, wind data records were also procured for purposes of estimating the return period of typhoon Imbudo from an anemometer based at Waglan Island, an island that is open to winds from the sea.

Correction factors relating the Waglan Island anemometer at 82.1 m to 200 m in the free stream have been determined by Hitchcock, *et al.* (2003), who performed a wind tunnel study of the island. Typhoon wind records were collected from 1953 to 1999, corrected to 200 m in the free stream, the resulting hourly mean wind speeds of which were analyzed by Holmes, *et al.* (2001) using the peaks-over-threshold approach. Based on the peaks-over-threshold parameters for an hourly mean wind speed of approximately 22 m/s, the return period of typhoon Imbudo was estimated to be slightly less than 1 year.

For typhoon Dujuan, the lowest instantaneous mean sea-level pressure measured in Hong Kong by HKO was 972.1 hPa. The maximum 10-minute mean wind speed was 25.9 m/s and the maximum 3-second gust wind speed was 32.5 m/s measured on September 2 at Stonecutters Island. The wind direction varied from 140 to 350, which is consistent with the eye of typhoon Dujuan passing to the north of Hong Kong.

The methodology used to calculate the return period of typhoon Imbudo was also employed for typhoon Dujuan. The maximum hourly mean wind speed determined at Waglan Island during typhoon Dujuan was approximately 23 m/s. Based on the peaks-over-threshold parameters from Holmes, *et al.* (2001), typhoon Dujuan was estimated to have a return period of 1 year.

4. Natural periods of vibration

4.1. Field measurements of building C and building E

Natural periods of vibration were estimated from power spectra obtained from a Fast Fourier

Transform of digital acceleration records measured during the two typhoons. The 10-minute acceleration records used spanned about two hours in duration for each typhoon, during periods which buildings C and E experienced their maximum peak accelerations. The natural frequency estimates are within 1% of natural frequency estimates previously determined using 100 ensemble averages and 32,768 FFTs applied to 12 hour records measured during typhoon Imbudo. Other details on how the natural periods for the different modes of vibration were determined can be found in Campbell, *et al.* (2005). A summary of the measured natural periods for both structures is presented in Table 1.

Table 1 Measured natural periods of building C and building E

Building	Natural Period (s)		
	Mode 1	Mode 2	Mode 3
C	3.26	3.19	1.86
E	2.80	2.72	1.72

4.2. Natural period predictors

The database of field tested buildings in Hong Kong, despite the prevalence of some of the tallest buildings in the world, is disappointingly small. A number of the landmark buildings have been tested and documented in the literature, however, a multitude of tall RC residential buildings have not.

A comparison between field measurements of buildings C and E during both typhoons to some relevant and common natural frequency predictors (Ellis 1980, Lagomarsino 1993, Tamura, *et al.* 2000, and Su, *et al.* 2003) has been presented in detail in Campbell, *et al.* (2005). The differences between field measurements and the natural frequency predictors indicated that the buildings that are the subject of the current study are generally stiffer than might be expected for other international buildings of similar height.

The beginnings of a database of Hong Kong buildings has been compiled from the documented studies of 15 tall buildings by Ko and Bao (1985), Su, *et al.* (2003), Campbell, *et al.* (2005), and other unpublished work by the authors. The available Hong Kong database can then be compared with the empirical-based predictors proposed by Ellis (1980) and Tamura, *et al.* (2000) that are both a function of building height (H), in metres.

Ellis (1980) proposed the empirical predictor in Eq. (1), based on the results of measurements taken on 162 multi-storey buildings, to estimate the natural period of the first mode of vibration of rectangular plan buildings. The predictor suggested by Ellis (1980) is a popular one that has received support by inclusion into the Code of Practice on Wind Effects in Hong Kong 2004 (CPWEHK-2004), the Australian and New Zealand Standard AS/NZS 1170.2 (2002), and the Eurocode ENV1991-2-4 (1994).

$$T = H/46 \quad (1)$$

More recently, Tamura, *et al.* (2000) suggested Eq. (2) for RC structures for habitability levels of acceleration and deflection, based on field measurements taken in Japan.

$$T_1 = H/67 \quad (2)$$

Fig. 2 presents the measured natural periods for this collection of tall buildings. The natural

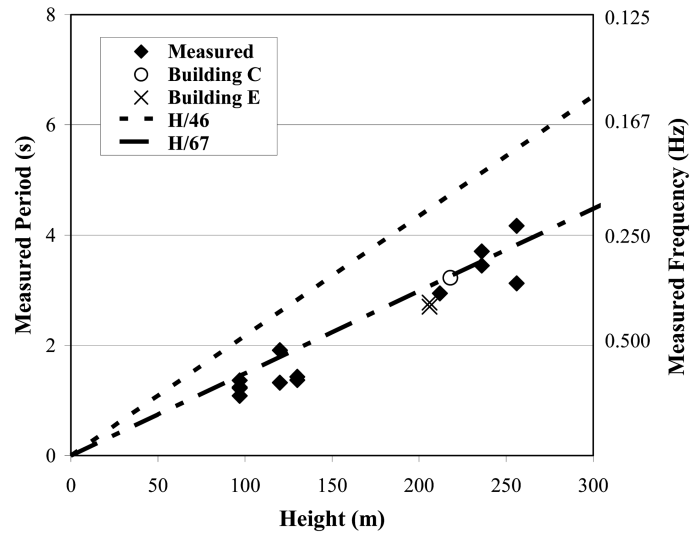


Fig. 2 Comparison of measured natural periods of vibration of tall buildings with empirical predictors $H/46$ and $H/67$

periods of the buildings studied so far are in better agreement with the empirical values suggested by $H/67$. The larger range of taller buildings used by Tamura, *et al.* (2000) to derive the suggested equation corresponds better to the tall RC buildings that have been measured in this study. This conclusion also suggests that the natural periods of tall RC buildings in Hong Kong are similar to tall RC buildings in the Japanese database, which may be attributed in part to the requirements in both regions to resist typhoon loading.

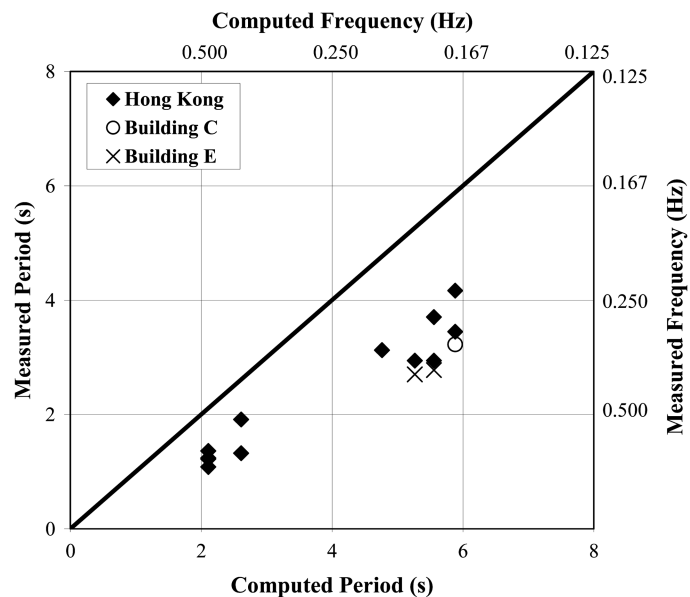


Fig. 3 Comparison of measured and predicted natural periods of vibration

Computational dynamic analyses were conducted by structural engineering consultants for some of the tested buildings in Hong Kong as part of their design process and before construction. The measured natural periods of RC buildings were generally lower than the computed natural periods, as shown in Fig. 3.

5. Structural damping

The capability of a tall building to dissipate vibrational energy is, for engineering purposes, most conveniently quantified as an overall value of structural damping that is most often modelled or considered as an “equivalent” viscous damping. The true nature of damping in tall buildings is actually more complex, depending on the amplitude of vibration, material properties, structural system and other factors and it is very difficult for the designer to predict with great certainty.

Jeary (1986) distinguished three amplitude zones from observed damping behaviour, namely a low-amplitude region, a region of increasing damping with amplitude, and a high-amplitude region. The low-amplitude region can be defined by a plateau where damping is proportional to the natural period of the structure and is predominantly caused by friction between structural joints and connections. The region of increasing damping with amplitude is caused by the progressive mobilization of macro- and micro-slippages in the structure. Finally, the high-amplitude region is demarcated as a plateau where all energy dissipative mechanisms have been mobilized causing a value of structural damping that essentially remains constant even for greater amplitudes of vibration.

Due to the relatively low return period of the typhoons during which the current measurements were taken, it was expected that the ensuing structural damping would correspond to the region of low-amplitude damping.

5.1. Random decrement technique

Determination of damping values from actual structures can be obtained through a number of techniques. Popular techniques of estimating damping values include: logarithmic decrement, autocorrelation, half-power bandwidth, and random decrement. For this study the random decrement technique (RDT) has been selected because of its advantages over the other techniques.

The RDT was first proposed and used by Cole (1973) for failure detection and damping estimation in aerospace structures. The RDT is a time-domain method by which an estimate of the free-decay response of a vibrating structure can be obtained, which in turn can be used to estimate its damping. The essence of the RDT is the calculation of the random decrement signature (RDS), which involves obtaining a time-history of a response process, then selecting segments of the time-history which, when ensemble averaged, removes the effects of initial velocity and random input. The resulting RDS approximates the free-decay vibration of the system, which can then be used to estimate modal parameters such as structural damping.

The main advantages of using the RDT to determine damping values over other methods are that it overcomes limits of stationarity, input amplitude and resolution, and allows for the convenient estimation of amplitude-dependence. For this reason, the RDT has been employed as the most suitable method to calculate damping of tall buildings under ambient excitation.

There are several issues that need to be addressed when using the RDT for estimating damping values from the limited data available from relatively short-lived phenomena, such as typhoons.

These issues fall into the categories of RDT applicability and appropriate calculation of the RDS, which includes the proper extraction of damping.

The RDT is applicable to vibrations when the system and the signal meet the following requirements. The system must have a single-degree-of-freedom with linear or only small non-linear behaviour (Ibrahim 1977). As well, the excitation input must be Gaussian, white noise, with zero mean, ensuring that the RDS is proportional to the autocorrelation function (Vandiver, *et al.* 1982 and Spanos and Zeldin 1998). In practice, this condition can be satisfied when a mode of vibration is isolated using a band-pass filter that is wider than the bandwidth of the response and provided that the band-pass filtered response is much narrower than the bandwidth of the entire acquired response (Vandiver, *et al.* 1982, Spanos and Zeldin 1998, Kijewski and Kareem 2000). However, the use of windowing to suppress side lobe leakage is discouraged as it effectively increases the bandwidth, and hence variance, of the process (Kijewski and Kareem 2002).

Proper calculation of the RDS can be performed in a number of ways depending on the selected trigger conditions. The RDS is typically calculated using Eq. (3) (Spanos and Zeldin 1998);

$$\bar{D}_{X_0}(\tau) = \frac{1}{N} \sum_{r=1}^N \eta_{X_0}(x_r) x_{r+\tau} \tag{3}$$

where:

\bar{D}_{X_0} = the estimate of the RDS at X_0 ;

$$\eta_{X_0}(x) = \begin{cases} 1, & x \in [X_0 - \Delta x, X_0 + \Delta x] \\ 0, & \text{otherwise} \end{cases} = \text{the trigger condition at the reference amplitude, } X_0;$$

Δx = the reference amplitude tolerance, defined as the size of the acceptance interval about X_0 , necessary for selecting discrete data;

τ = the time lag over which the RDS is calculated;

N = the total number of data points that satisfy the trigger conditions (i.e. the total number of segments); and

r = segment number.

An effective trigger condition, satisfying requirements of both amplitude and slope, is to select the peaks of the process that lie within a narrow range of each selected reference amplitude of vibration, which is defined as the reference amplitude tolerance, Δx . This can be formulated, for example, as $\Delta x = X_0 \pm 0.03 X_0$, where the reference amplitude tolerance is $\pm 3\%$ of the reference amplitude. The selected amplitude is defined as the reference amplitude for which a single value of damping is calculated. Amplitude-dependent effects can be quantified conveniently when such a triggering condition is used (Tamura and Suganuma 1996). The trigger condition used in this study identifies peaks in the time-history that satisfy the selected reference amplitude of vibration. The subsequent RDS is then used to determine damping at the reference amplitude, allowing for amplitude-dependent effects to be quantified when damping estimates at multiple reference amplitudes are compared. Because the probability of an exact peak being located at the reference amplitude is low, a range around the reference amplitude, rather than the reference amplitude itself, is selected. This range, defined by the reference amplitude tolerance, Δx , effectively increases the number of peaks that satisfy the trigger condition.

A test was performed to determine the effect of the number of segments, N , on the variation of damping values obtained from the RDS. Large changes in the calculated damping value are

observed for $N < 200$, corresponding to a large uncertainty in the actual damping value, whereas for $N \geq 200$ the calculated damping value became stable indicating that the result was independent of N . Kijewski & Kareem (2000) suggest that the minimum number of N is 200. For shorter records, Kijewski and Kareem (2000) demonstrated that N may be increased by using overlapping segments without significantly affecting the RDS. Details of this test can be found in Campbell (2005).

Another test, also outlined in Campbell (2005), was performed to determine an appropriate reference amplitude tolerance that would effectively increase the number of segments used in generating the RDS while without compromising the amplitude-dependent effects. The value of Δx was varied from ± 0.01 to ± 0.08 of the reference amplitude, in 0.01 increments. For a tolerance of ± 0.01 the number of segments, N , was always below 200 at all tested reference amplitudes. As the tolerance incrementally increases to ± 0.08 the number of segments increases, as expected. Using a tolerance of ± 0.08 , however, is not a strict enough trigger condition because it incorporates too large a range of peaks, compromising the accuracy of the RDS and obscuring possible amplitude-dependent effects of damping. For this reason, Tamura and Suganuma (1996) suggest a tolerance of ± 0.03 of the reference amplitude. However, using this tolerance level produced too few segments from the time-histories collected during both typhoons. The transient nature of typhoons can often cause non-optimal conditions for the acquisition and analysis of building vibrations. Under the conditions that occurred during typhoons Imbudo and Dujuan, the amplitude of vibrations combined with their short durations made amplitude-dependent analyses difficult. Therefore, a compromise between obtaining a minimum number of segments and the ability to generate an accurate RDS resulted in the selection of a reference amplitude tolerance level of ± 0.05 , which was used for all RDT calculations in this study.

Cole (1973) notes that when extracting segments for the RDS calculation using positive and negative reference amplitudes that are significantly lower or higher than the standard deviation (S.D.) of the signal tend towards becoming correlated, biasing the RDS. In this study, it was noted that as the reference amplitudes approached values significantly lower or higher than the S.D. value (i.e. $\pm 1 \times \text{S.D.}$), N generally decreased to below 200. Since damping estimates were only calculated for RDSs with $N \geq 200$, data that were biased were excluded. Therefore, the trigger condition employed in the current study incorporates both positive and negative peaks to increase the number of segments caused by short duration time-histories.

It has been observed by Kijewski and Kareem (2000) that the variance of the RDS increases with an increase in the time lag. Conversely, more confidence is gained from estimates of damping when greater numbers of cycles are used. When more cycles are included in the estimation of damping, the amplitudes of these subsequent cycles may decrease to a level below that of the selected reference amplitude which may span regions of amplitude-dependency, masking its presence and invalidating the estimated damping value. Therefore, a compromise between the effects of time lag and number of cycles is to estimate damping over 5 cycles (Caldwell 1978 and Kijewski and Kareem 2000).

Through mathematical and numerical investigation, Huang and Yeh (1999) revealed some properties of RDSs that advanced the theoretical basis of the RDT. Notably, Huang and Yeh (1999) showed that without *a priori* knowledge of the applied forcing functions, conclusions about extracted modal parameters may be biased. This bias is revealed through the presence of a singular point at the beginning of the acceleration RDS which, theoretically, increases the variance of the RDS as well as prevents equivalence between the RDS and the free decay response. However, it is also shown that this singular point does not exist for displacement or velocity measurements. Continuing on a theoretical basis, Ku, *et al.* (2006) developed an approach for parameter identification from acceleration

measurements based on RDT, FFT algorithms and a linear least squares procedure. Ku, *et al.* (2006) stated that the application of the RDT to displacement or velocity measurements should be a reliable alternative to using acceleration measurements. However, the measurement resolution and accuracy of currently available displacement and velocity sensors are significantly less than accelerometers and insufficient to investigate amplitude dependent effects.

In practical applications of the RDT to field measurements of wind-induced building acceleration, it is uncertain that the singular behaviour will become manifest or to what degree its effects will bias the RDS. To test the applicability of the RDT to acceleration measurements similar to those obtained in field measurements, a wind tunnel test was performed on an aeroelastic tall building model. During the test, measurements of acceleration and equivalent displacement in the cross-wind direction of motion were taken at the same point near the top of the model with an accelerometer and strain gauges, respectively. Because measurements of acceleration and displacement were taken simultaneously, this allowed for the direct comparison of damping estimates obtained from both acceleration and displacement results. The free decay vibration of the aeroelastic model prior to testing yielded a damping value of 0.87% of critical in the cross-wind direction and was verified for three samples.

Damping was determined from the RDT analysis procedure detailed above at 23 equivalent amplitudes of acceleration and displacement. An example of the comparison of different damping estimation techniques is presented in Fig. 4. In this figure, the acceleration and displacement time-histories are provided along with the line-of-best-fit for peak values determined from the RDSs and

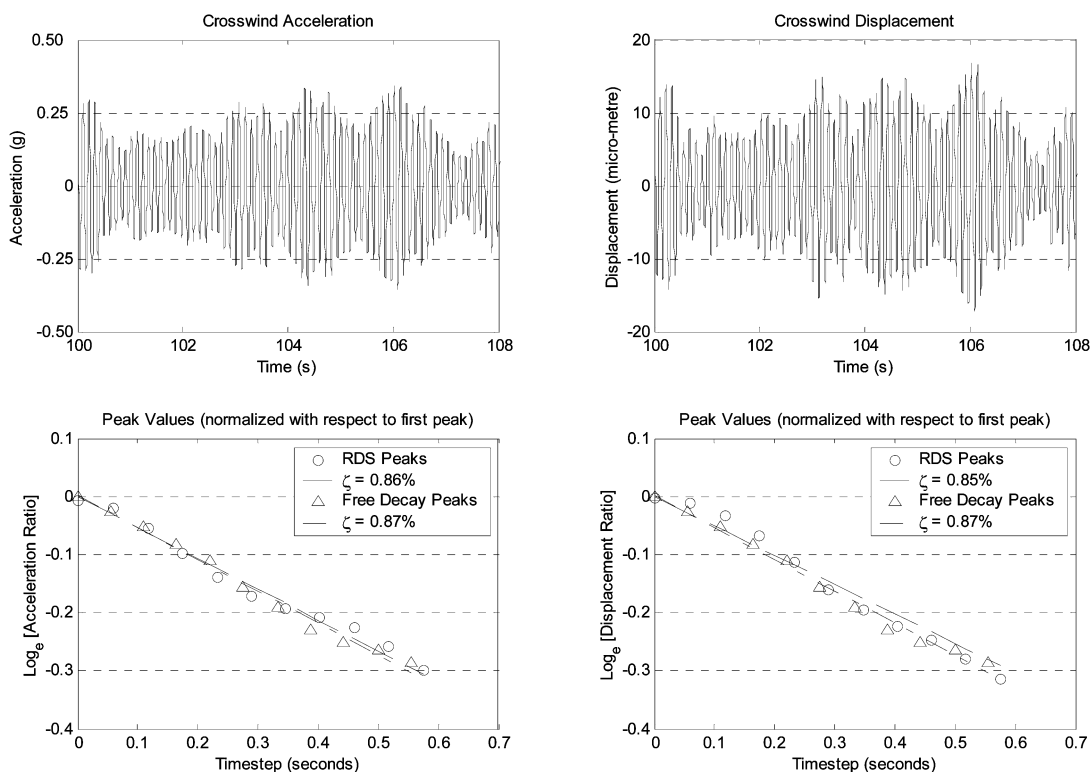


Fig. 4 Comparison of damping estimation techniques

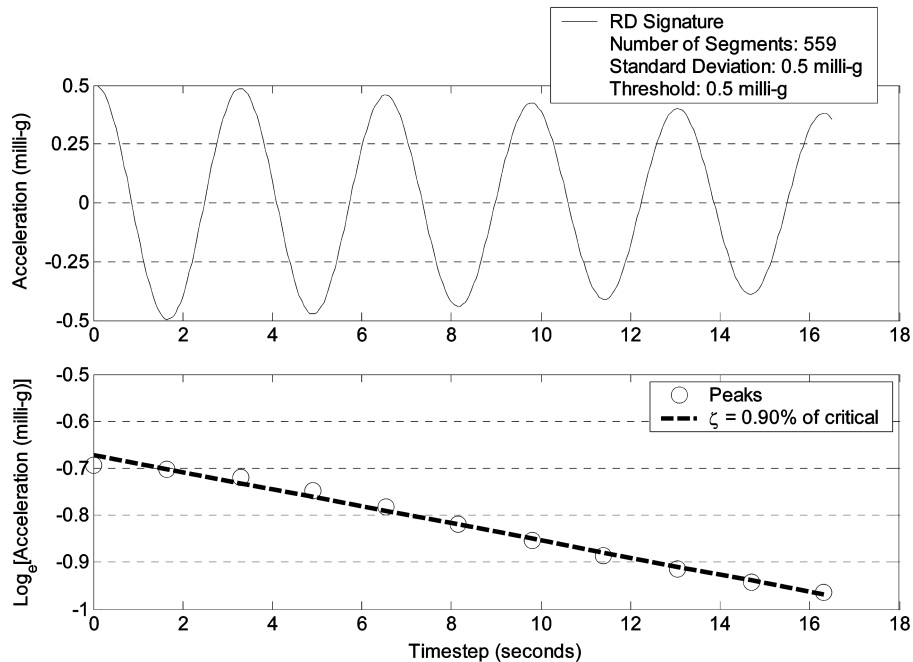


Fig. 5 Estimation of damping using RDT for building C: random decrement signature (top) and logarithmic decrement

the free-decay vibration. For the entire study, the average estimates of damping from the 23 samples are 0.80% of critical from acceleration measurements and 0.82% of critical from displacement measurements, which are less than 8% from the value determined through free-decay vibration. If the number of segments is raised to $N=1,000$, the average estimates of damping from 10 amplitudes are 0.82% of critical from acceleration measurements and 0.86% of critical from displacement measurements, which are less than 6% from the value determined through free-decay. In this study, the potential effects of bias in the RDS obtained from acceleration measurements could not be confidently ascertained. In practice, the presence and effects of the singular behaviour with RDT may not be significant, allowing for reasonable and practical estimates of damping to be obtained from acceleration measurements.

Once a RDS is obtained, a damping value can be estimated using, for example, a linear least-squares fit of the logarithm of peak values. An example of a damping value calculated from the RDT using the above-mentioned protocol is presented in Fig. 5 for field measurements of Building C during one typhoon.

5.2. Damping measurements

Damping values were estimated using the RDT for buildings C and E using contiguous records capturing the peak response periods during both typhoons. Strong winds associated with the movement of typhoon Imbudo past Hong Kong allowed approximately 6 hours of acceleration records to be used with the RDT. For typhoon Dujan, a total duration of 5 hours of acceleration data was used for each building. Damping values were calculated using the RDT at 50 acceleration amplitudes between a nominal zero value and 95% of the peak acceleration in that record. However, in

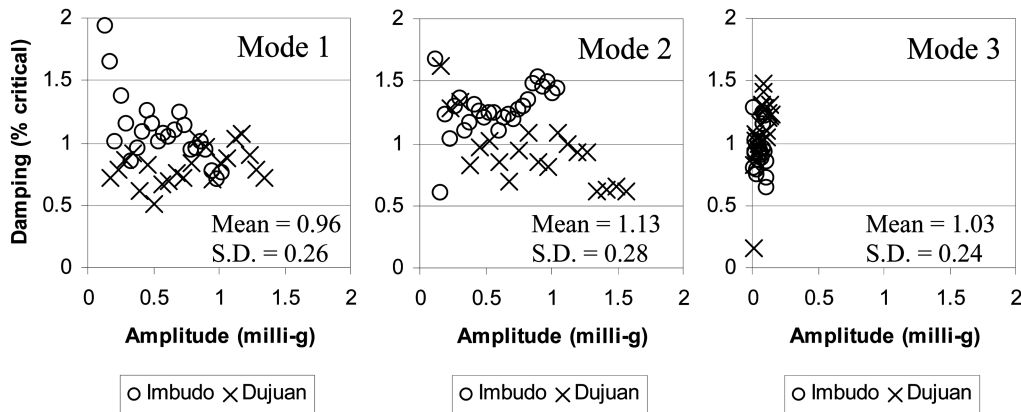


Fig. 6 Damping of building C during typhoons Imbudo and Dujan

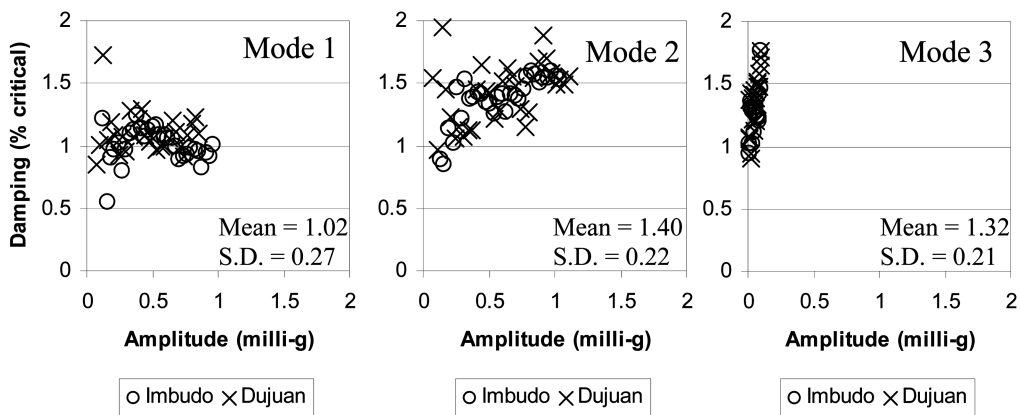


Fig. 7 Damping of building E during typhoons Imbudo and Dujan

accordance with previously outlined RDT protocol, only those damping values with $N \geq 200$ were used.

Figs. 6 and 7 present the calculated mean and standard deviation damping values for the first three modes of vibration of buildings C and E, respectively, during both typhoons. For both buildings, the amplitudes of acceleration measured for mode 3, i.e., predominantly torsional modes of vibration, are much smaller than those measured for the predominantly translational modes 1 and 2. In general, a high degree of variability exists in estimated damping values for the first three modes of vibration across the range of acceleration amplitudes observed. This variability is attributed to the complex motion of the response of the buildings caused by the uncontrolled ambient excitation.

Typhoons Imbudo and Dujan were approximately 1-year return period events. Hence, the estimated damping values are associated with the lower range of acceleration amplitudes where evidence of amplitude-dependent effects could not be confidently ascertained. As the buildings have been instrumented as part of a longer term monitoring study, it is anticipated that data collected from future strong wind events will facilitate a more rigorous assessment of any amplitude-dependent effects.

5.3. Evaluation of empirical damping predictors against measured values

One of the earliest predictors of the expected damping of a building was proposed by Davenport and Hill-Carroll (1986), given in Eq. (4), that was based on field measurements of damping on 165 buildings.

$$\zeta = A \left(\frac{\Delta}{H} \right)^n \quad (4)$$

In Eq. (4), Δ is the S.D. displacement amplitude (in millimetres), H is the height of the building (in metres), and A and n are constants based on building type (reinforced concrete or steel) and the number of storeys (two height classifications: 5 - 20 storeys or greater than 20 storeys). For RC buildings greater than 20 storeys A and n are 0.02 and 0.11, respectively. The subject buildings in this study, buildings C and E being 64 and 60 storeys respectively, are probably beyond the range of the experimental data upon which this damping predictor was based.

Values of structural damping predicted by Eq. (4) are relevant to lower amplitudes of vibration, particularly for serviceability considerations. No plateau regions indicative of an upper or lower limit to the amount of structural damping are acknowledged in this formulation and this damping predictor is not applicable to mode shapes dominated by torsional motion.

It should be noted that the S.D. displacement amplitude is used rather than the peak since the average damping energy dissipation for sinusoidal or random vibration (or vibration regimes with a peak factor between these two limits) with the same S.D. values will be at approximately the same level. In order to compare amplitudes of vibration with other damping estimators it was necessary to convert from S.D. displacement to peak displacement. In doing so, a peak factor of 3.3 was used for a 10-minute period.

Another relevant predictor proposed by Jeary (1986), which accounted for amplitude-dependent effects of damping, is presented in Eq. (5).

$$\zeta_j = \zeta_{0j} + \zeta_{1j} \left[\frac{x_H}{H} \right] \times 100 \quad (5)$$

where:

j = mode number;

$$\zeta_{01} = \frac{1}{T_0}, \text{ where } T_0 \text{ is the natural period of the first mode of vibration, and } \log_{10} \zeta_{11} = \frac{\sqrt{D}}{2}.$$

In Eq. (5), x_H is the absolute value of amplitude of vibration (in metres), H is the height of the building (in metres), and D is the dimension of the building (in metres) including the dimensions of any structures attached at the base of the building at ground level, aligned in the dominant direction of motion.

The first term in Eq. (5), ζ_{0j} , corresponds to a low-amplitude constant value dependent on the natural period of vibration of j^{th} mode, while the second term represents a linear rate of increase in damping with respect to amplitude of vibration, x_H . Instead of using $46/H$ to calculate ζ_{0j} for the first mode in this study, the actual natural frequency values were used which should result in closer predicted values of damping. The lower-amplitude damping plateau is effectively neglected in Eq. 5 and Jeary (1986) recommended an upper limit for structural damping of 5% of critical that was based on measurements of the response of buildings to earthquake excitation. A more recent study

by Tamura (2006) suggested that the maximum achievable structural damping for strength and safety design of wind resistant tall buildings will be significantly less than 5% of critical.

Lagomarsino (1993) proposed a predictor for low-amplitude vibration, i.e., below that where amplitude-dependent damping is engaged. Lagomarsino (1993) stated that the natural period is the only statistically relevant parameter that can be used to describe the initial first modal damping value, ζ_{0k} , and using a theoretical mechanism for energy dissipation, analogous to Rayleigh's damping law, proposed Eq. (6).

$$\zeta_{0k} = \alpha' T_k + \beta' / T_k \tag{6}$$

In Eq. (6), α' and β' are regression parameters based on whether the building is of steel, RC, or mixed construction, and T_k is natural period of the k^h mode. For RC buildings, α' and β' are 0.7238 and 0.7026, respectively.

In physical terms, the predictor presented by Lagomarsino (1993) lends itself to elastic deflection under low levels of displacement vibration and dissipative, elastic deflection under higher levels of displacement vibration caused by the progressive mobilization of macro- and micro-slippages. However, it is observed when using this predictor that damping values decrease as natural periods decrease, generally contradicting what has been measured in the field. This characteristic was also noted by Kareem and Gurley (1996).

Tamura, *et al.* (2005) has recently offered damping predictors for both steel and RC buildings. Based on a regression analysis performed of field measurements of the dynamic properties of 25 RC buildings in Japan, the structural damping predictor for a RC building is presented in Eq. (7).

$$\zeta_1 = \frac{0.014}{T_1} + 470 \frac{x_H}{H} - 0.0018 \tag{7}$$

In Eq. (7), x_H/H is the tip drift ratio (unitless) and T_1 is the natural period of the first mode of vibration (in seconds). In this equation, the natural period for serviceability considerations can be estimated from Eq. (2). However, it is convenient to replace the period of vibration term with height by substituting Eq. (2) into Eq. (7). This new equation is given as Eq. (8).

$$\zeta_1 = \frac{0.93}{H} + 470 \frac{x_H}{H} - 0.0018 \tag{8}$$

This predictor is applicable only for RC buildings and only to drift ratios satisfying $x_H/H \leq 2.0 \times 10^{-5}$ and $H < 100$ m. Although the heights of the subject buildings are beyond the range of applicability, the predictor in Eq. (8) still contains the largest number of taller buildings, compared to other predictors' databases, highlighting the lack of available damping data for tall buildings.

Comparisons of predicted damping values, based on natural periods that were determined from Eq. (2) where relevant, and measured damping values for translational modes of vibration are presented in Figs. 8 and 9 for buildings C and E, respectively. Approximating equivalent amounts of displacement from field measurements was performed by double-differentiating the acceleration RDS under the assumption that it is a sinusoidal vibration with equivalent viscous damping.

The predictor from Davenport and Hill-Carroll (1986) provides the closest agreement to the measured values of overall structural damping for buildings C and E. If used during the design stage, this predictor would provide damping values that are close to those that have been measured for these buildings. The predictor from Jeary (1986) begins as conservative (i.e. it tends to predict

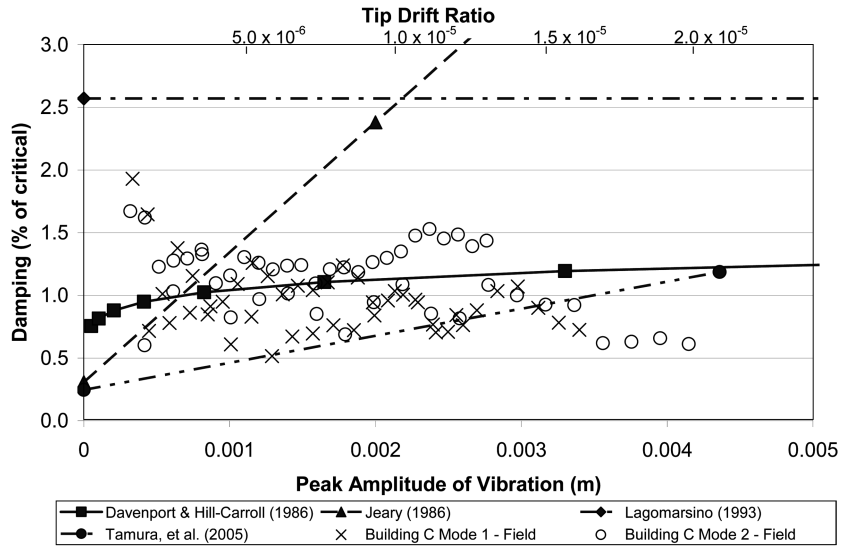


Fig. 8 Predicted and measured damping for 1st and 2nd translational modes for building C

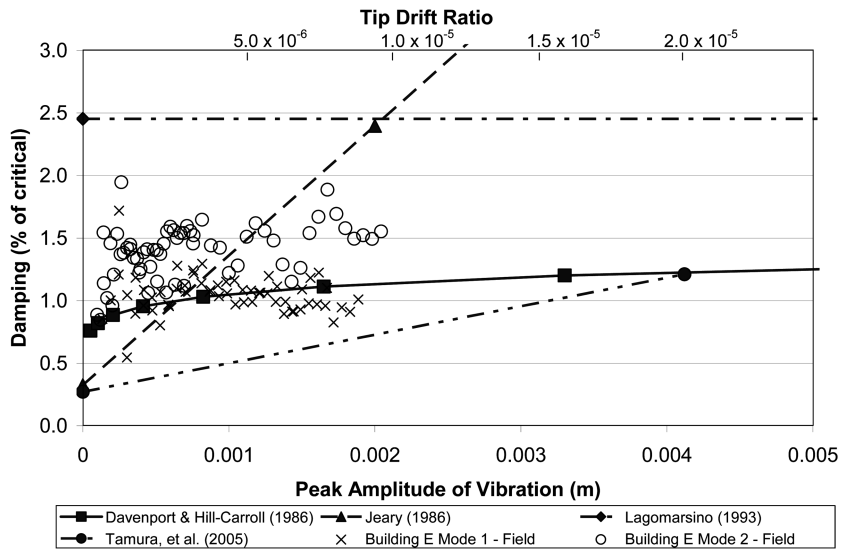


Fig. 9 Predicted and measured damping for 1st and 2nd translational modes for building E

structural damping values that are less than those determined from the full-scale acceleration measurements) and then quickly becomes non-conservative as the amplitude of vibration increases. In contrast, the Lagomarsino (1993) predictor is nonconservative and yielded structural damping values for the translational modes of vibration that were at least twice the measured values in the current study.

Predicted damping values from Tamura, *et al.* (2005) are mildly conservative compared to the measured values, except in the vicinity of displacements of the order of 0.003 to 0.004 m, which is approaching the tip drift ratio limit to which this predictor is applicable. Given that estimates of

measured damping values from the RDT are seen to vary by 20% it is felt that the predictor given by Tamura, *et al.* (2005) provides an appropriate estimate of damping for tall RC residential building design. Moreover, the largest number of taller buildings are included in Tamura, *et al.* (2005) supporting the use of this predictor to the buildings that are the subject of this study.

Kareem and Gurley (1996) noted that the databases on which some of the abovementioned damping predictors were based contained many of the same buildings. The majority of these were shorter buildings with the few taller ones being measured generally under small levels of vibration. While the predictors discussed above assume slightly different formulations, they are inevitably representative of the types of buildings that have been used in the database. Significant differences in empirical predictors may arise due to different construction methods and for this reason empirical predictors may reflect regional characteristics of buildings. While recognising that the current study is limited to two buildings, the similarity that has been observed between buildings in this study and those that are included in Tamura, *et al.* (2005) may be explained by requirements of Hong Kong buildings to resist typhoons and Japanese buildings to resist typhoons and earthquakes.

6. Effects of the variability of natural period and damping on alongwind response

It is well known that natural period and damping are important design parameters that affect the overall wind-induced response of a tall building. At the design stage, natural periods are commonly overestimated by computational models while it is apparent that structural damping values included in design codes and standards currently overestimate damping levels in tall buildings. To assess the potential effects of the variation of these two parameters the gust response factor (GRF) approach, which has been adopted by most current international wind loading design codes and standards, has been used to characterize the alongwind dynamic loads of buildings C and E through the calculation of the GRF.

GRFs were calculated for four different sets of values labelled as Set 1 through to Set 4. These sets are based on values that building C or E took during their design and construction, starting first with values suggested by the local wind loading code, CPWEHK-2004 (Set 1), but with a revised value of structural damping of 1% of critical, which is more applicable to serviceability conditions. The values in Set 2 are those used during the wind tunnel test, where the natural periods were estimated from a computational model and the structural damping is taken as 1% of critical. The values in Set 3 were determined using the most appropriate predictors for serviceability-level vibrations, which were those from Tamura, *et al.* (2005). Finally, Set 4 comprises natural periods as determined from the field measurements for both buildings and mean damping ratios corresponding to the first two translational modes of vibration for each building.

The GRFs were calculated for a 10-minute duration, which is considered to be appropriate for serviceability-level accelerations, for considering occupant comfort for example, to avoid the potential masking of effects that may occur if longer durations, such as 1 hour, are used. Consequently, several parameters required modification. The peak factor of the background response was modified to a value of 3.0 for a 10-minute period using ESDU 83045 (1983). The peak factor of the resonant response was calculated using Eq. (9).

$$g_f = \sqrt{2 \log_e(600 \cdot \nu)} \quad (9)$$

In Eq. (9), ν is the mean value crossing rate (in Hertz). The 10-minute mean wind speed at the top of each building was approximately equal to 30 m/s, corresponding to a 1 year return period to be consistent with the wind events during which the full-scale measurements were taken.

Damping values for Set 3 were determined from the Tamura, *et al.* (2005) predictor using a tip drift ratio of $x_H/H = 2.0 \times 10^{-5}$, the largest tip drift ratio for which the predictor is valid.

The calculated 10-minute GRFs have been normalized with respect to Set 1 and are presented in Table 2.

Table 2 Normalized 10-minute dynamic magnification factors (CPWEHK-2004)

	Building	Mode	Set 1	Set 2	Set 3	Set 4
	C	1	1.00	1.06	0.94	0.94
		2		1.04	0.94	0.95
	E	1	1.00	1.08	0.94	0.94
		2		1.05	0.94	0.92

Set	Building	Natural Period (s)		Damping (% of critical)		
1	C	4.74	$H/46$	1.00	[CPWEHK-2004]	
	E	4.48	[CPWEHK-2004]			
2	C	6.25	5.69	1.00	used in wind tunnel test	
	E	6.46	5.66			
3	C	3.25	$H/67$	1.19	$\left(\frac{0.93}{H} + 470\frac{x_H}{H} - 0.0018\right) \times 100$	
	E	3.07	[Tamura, <i>et al.</i> (2000)]	1.21		[Tamura, <i>et al.</i> (2005)]
4	C	3.19	3.26	1.13	0.96	measured
	E	2.80	2.72	1.02	1.40	
		X	Y	X	Y	

The majority of normalized GRFs presented in Table 2 are close to a value of unity. The largest GRFs, 4% - 8% larger than Set 1, were calculated for Set 2 whose natural period values were used for the wind tunnel test. The GRF values for building C and E in Set 2 are larger than Set 1 by about 4% to 8%, which is the result of the much higher natural periods. A decrease in the GRF of 6% is observed for Set 3 and a decrease of 5% - 8% is observed for Set 4. That the results from Set 3 and Set 4, whose natural frequencies and damping values are derived from empirical and measured sources, respectively, are only 8% smaller than those values estimated by Set 1 is entirely fortuitous and due to the effects of predictors overestimating natural period offsetting the effects of overestimating structural damping.

It is well established that damping values under serviceability conditions are lower than that under permissible stress/ultimate limit state conditions. However, in most codes, except AS/NZS 1170.2 (2002) and AIJ 2005, there are no provisions for applying damping values for serviceability conditions. Damping values suggested in codes and standards are generally higher than the values measured in tall buildings, as seen in Fig. 10, partly because the higher values are more relevant to design requirements and partly because measurements taken so far in tall buildings rarely reach amplitudes associated with design events. Nevertheless, the damping values measured for buildings C and E are believed to be representative for tall buildings for serviceability considerations, including occupant comfort assessment.

The sensitivity of the alongwind response of these two buildings to changes in natural periods and damping values is analyzed using a systematic approach while retaining a serviceability-level wind speed of 30 m/s at building height. Figs. 11 and 12 give the 10-minute GRFs calculated for the first mode of buildings C and E using the GRF approach. Natural periods were varied from -25% to 75% from the actual measured value, T_0 , in 25% intervals, corresponding to differences between actual buildings and their FEM models observed by Su, *et al.* (2003) and Campbell, *et al.* (2005). Structural damping values were varied according to selected nominal values of 0.50%, 0.75%, 1.00%, 1.50%, and 2.00% of critical damping. The lower damping values in this range are relevant to that encountered for serviceability-level vibrations of tall RC buildings. As a reference, damping values of 1.50% and 2.00% of critical are also included, however, these are generally considered to be higher than that found in conventional tall RC buildings in serviceability conditions. Some

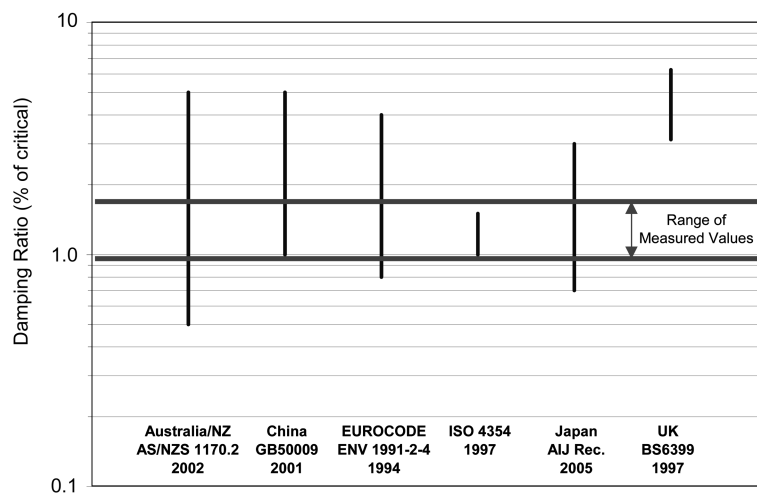


Fig. 10 Suggested damping ratio ranges for selected international codes and range of measured damping values for building C and building E

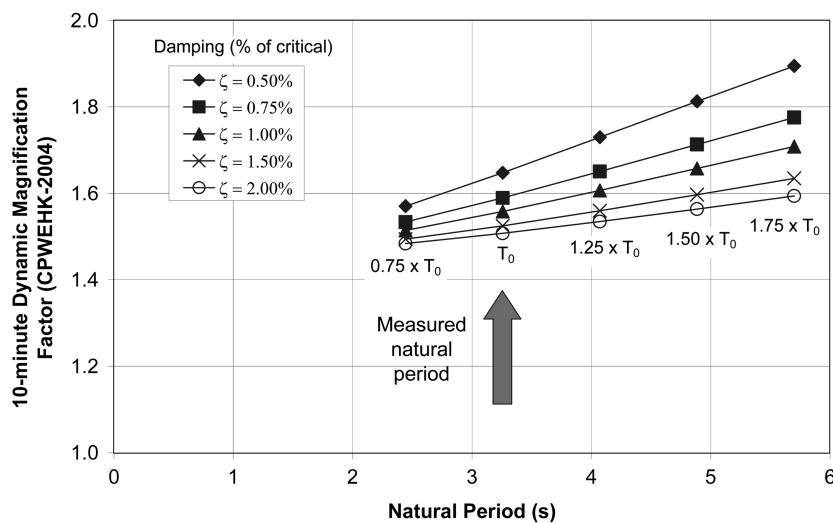


Fig. 11 10-minute dynamic magnification factor for varying natural period and damping for building C

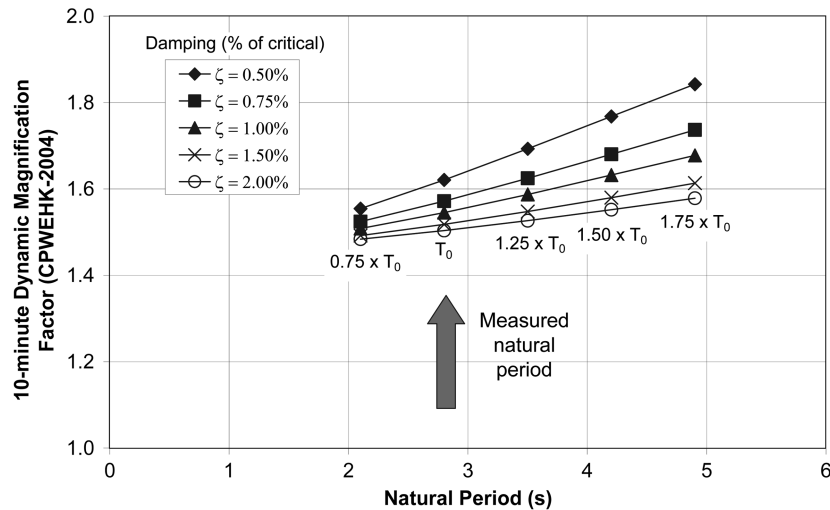


Fig. 12 10-minute dynamic magnification factor for varying natural period and damping for building E

building codes suggest a damping value of 2.00% of critical for strength design, for example, but give no explicit instructions as to how these values should or should not be used for serviceability design. For the purposes of the following calculations it is assumed that these buildings are operating at a reduced velocity of less than 6, typical of serviceability conditions.

The resulting 10-minute GRFs for buildings C and E, presented in Figs. 11 and 12, demonstrate the effects of underestimating natural period, overestimating structural damping, or a combination thereof, that may cause larger GRFs than were anticipated during design. Figs. 11 and 12 illustrate that going from a natural period of $0.75 \times T_0$ to T_0 causes an increase in GRF of approximately 2% to 5% for damping values between 0.5% and 2.0% of critical, respectively.

Damping values that are taken from current building design codes and standards for serviceability levels may be overestimated, and therefore, nonconservative. A change in damping value from 2.0% to 0.50% of critical equates to an increase in GRF of approximately 5% at a natural period of $0.75 \times T_0$, 8% at T_0 , and 17% at $1.75 \times T_0$. The effect of overestimating damping values at large natural periods is greater than that at lower natural periods partly because of the increase in energy in the alongwind wind velocity spectrum at higher periods. It is noteworthy that these changes in the GRF are quite modest compared with the relatively large changes in damping values. A comparison between the relative contributions of background and resonant components indicates that at lower natural periods the background component dominates. For example, even at the measured natural periods for a damping value of 1.00% of critical for these two buildings, the contribution from background excitation is approximately twice that of the resonant excitation. In cases where the background component of excitation dominates, differing damping values cause only moderate changes to the GRF. On the other hand, damping values are more critical to the alongwind response when the resonant component of excitation dominates.

7. Conclusions

Field measurements of wind-induced vibrations have been performed on two reinforced concrete buildings that are among the tallest residential buildings in the world. The dynamic properties of

these tall buildings have been compared with common and relevant empirical predictors for natural period and structural damping. This comparison is especially important as the amount of information known about the dynamic parameters of buildings of these heights is very limited.

A collection of field measurements conducted on a number of tall buildings in Hong Kong have been found to follow the empirical natural period predictor of $H/67$, suggested by Tamura, *et al.* (2000) as opposed to the more common $H/46$, suggested by Ellis (1980). These results suggest that tall, reinforced concrete buildings in Hong Kong, which are primarily designed to resist typhoons, share a similar natural period to height relationship of $H/67$ applicable to buildings in Japan, which are designed to resist both typhoons and earthquakes. It has also been shown that structural damping values for serviceability-level vibrations of these two buildings, which are representative of current design trends in tall reinforced concrete residential buildings in Hong Kong, are generally lower than those suggested by international design codes and standards. Conservatively, the damping values of these buildings may be estimated by the empirical predictor proposed by Tamura, *et al.* (2005).

The effects of varying natural frequency and structural damping values on the alongwind response for these two buildings have been studied with respect to serviceability-level vibrations. For typical tall building designs using a gust response factor approach, reasonable predictions of wind-induced loads have probably been achieved through the somewhat fortuitous offsetting of the effects of overestimating both natural periods and structural damping values. Generally, natural periods estimated computationally are higher than those measured in actual buildings. This has the effect of decreasing the gust response factor. In cases where the background component of alongwind excitation dominates, differing damping values cause only moderate changes to the gust response factor.

Acknowledgements

Kowloon Properties Co. Ltd., MTR Corporation Limited, Wong & Ouyang (Civil-Structural Engineering) Ltd., and Hip Hing Construction Co. Ltd. must be thanked for their cooperation in testing these buildings. The staff of the CLP Power Wind/Wave Tunnel Facility is thanked for their assistance during these tests.

Acknowledgment also goes to the Highways Department of the Hong Kong, S.A.R. who provided wind data from the Stonecutters Island anemometer.

This research project is funded by the Research Grants Council of Hong Kong (Project HKUST6222/01E). The financial support is gratefully acknowledged.

References

- AS/NZS 1170.2. (2002). Australian/New Zealand Standard, Structural design actions, Part 2: Wind actions. Standards Australia & Standards New Zealand.
- Caldwell, D.W. (1978), "The measurement of damping and the detection of damage in linear and nonlinear systems by the random decrement technique", Diss. University of Maryland, U.S.A.
- Campbell, S. (2005), "Full-scale measurements of wind-induced building motion", MPhil Dissertation, The Hong Kong University of Science and Technology.
- Campbell, S., Kwok, K.C.S., and Hitchcock, P.A. (2005), "Dynamic characteristics and wind-induced response of two high-rise residential buildings during typhoons", *J Wind Eng. Ind. Aerodyn.*, **93**, 461-482.
- Code of Practice on Wind Effects in Hong Kong. (2004), Buildings Department of the Government of the Hong Kong SAR.
- Cole, H.A., Jr. (1973), "On-line failure detection and damping measurement of aerospace structures by random decrement signatures", NASA CR-2205, March.

- Davenport, A.G., and Hill-Carroll, P. (1986), "Damping in tall buildings: Its variability and treatment in design", *Proceedings of Building Motion in Wind, a session of the ASCE Convention*, Seattle, Washington, April 8, 1986, pp. 42-57.
- Ellis, B.R. (1980), "As assessment of the accuracy of predicting the fundamental natural frequencies of buildings and the implications concerning the dynamic analysis of structures", *Proceedings of the Institution of Civil Engineers*, Part 2, vol. **69**, Sept., 763-776.
- Engineering Sciences Data Unit (ESDU) (1983), "Strong winds in the atmospheric boundary layer, Part 2: discrete gust speeds", vol. 83045.
- Eurocode ENV1991-2-4. (1994), EUROCODE 1: Basis of Design and Actions on Structures, Part 2.4: Wind Actions, CEN/TC 250/Sc1.
- Huang, C.S., and Yeh, C.H. (1999), "Some properties of random dec signatures", *Mechanical Systems and Signal Processing*, **13**(3), 491-507.
- Hitchcock, P.A., Kwok, K.C.S., and Yu, C.W. (2003), "A study of anemometer measurements at Waglan Island, Hong Kong", Technical Report WWTF002-003, HKUST.
- Holmes, J.D., Hitchcock, P.A., Kwok, K.C.S., and Chim, J.K.S. (2001), " Re-analysis of Hong Kong typhoon wind speeds using the 'peaks over threshold' approach", *Proceedings of Fifth Asia-Pacific Conference on Wind Engineering* (Kyoto, Japan, 2001) Elsevier B.V., pp. 357-360.
- Ibrahim, S.R. (1977), "Random decrement technique for modal identification of structures", *J. Spacecraft*, **14**(11), 696-700.
- Jeary, A.P. (1986), "Damping in tall buildings – A mechanism and a predictor", *Earthq. Eng. Struct. Dyn.*, **14**, 773-750.
- Kareem, A., and Gurley, K. (1996), "Damping in structures: its evaluation and treatment of uncertainty", *J. Wind Eng. Ind. Aerodyn.*, **59**, 131-157.
- Kijewski, T., and Kareem, A. (2000), "Reliability of random decrement technique for estimates of structural damping", *8th ASCE Specialty Conference on Probabilistic Mechanics and Structural Reliability*, pp. 294-299.
- Kijewski, T., and Kareem, A. (2002), "On the reliability of a class of system identification techniques: insights from bootstrap theory", *Structural Safety*, **24**, 261-280.
- Ko, J.M., and Bao, Z.W. (1985), *Ambient Vibration Measurements on Existing Tall Buildings in Hong Kong*. Hong Kong Polytechnic.
- Kwok, K.C.S. (1992), "Natural frequencies of vibration and damping ratios of tall buildings and structures", *Proceedings of 2nd International Conference on Highrise Buildings*, Nanjing, 396-401.
- Ku, J.K., Cermak, J.E., and Chou, L.-S. (2006), "Random decrement based method for modal parameter identification of a dynamic system using acceleration responses", *J. Wind Eng. Ind. Aerodyn.*, doi:10.1016/j.jweia.2006.08.004 (in press)
- Lagomarsino, S. (1993), " Forecast models for damping and vibration periods of buildings", *J. Wind Eng. and Ind. Aerodyn.*, **48**, 221-239.
- Mercer Human Resource Consulting. Cost of Living Survey (2005) – Worldwide Rankings, Online source: <http://www.mercerhr.com>, 2006.
- Spanos, P.D. and Zeldin, B.A. (1998), "Generalized random decrement method for analysis of vibration data", *Trans. of the ASME*, **120**, 806-813.
- Su, R.K.L., Chandler, A.M., Lee, P.K.K., To, A., and Li, J.H. (2003), "Dynamic testing and modelling of existing buildings in Hong Kong", *Hong Kong Inst. of Eng. Transactions*, **10**(2), 17-25.
- Tamura, Y (2006), "Amplitude dependency of damping in buildings and estimation techniques", *12th Australasian Wind Engineering Society Workshop*, Queenstown, New Zealand, Feb 2-3, 2006.
- Tamura, Y., and Suganuma, S.-Y. (1996), "Evaluation of amplitude-dependent damping and natural frequency of buildings during strong winds", *J. Wind Eng. Ind. Aerodyn.*, **59**, 115-130.
- Tamura, Y., Suda, K., and Sasaki, A. (2000), " Damping in buildings for wind resistant design", *Proc. Int'l Symp. on Wind and Structures* (Cheju), Techno-Press, Korea, pp.115-130.
- Tamura, Y., Yoshida, and A., Zhang, L. (2005), " Damping in buildings and estimation techniques", *6th Asia-Pacific Conference on Wind Engineering*, Seoul, S. Korea, Sept 12-14, 2005, pp. 193-214.
- Vandiver, J.K., Dunwoody, A.B., Campbell, R.B., and Cook, M.F. (1982), "A mathematical basis for the random decrement vibration signature analysis technique", *J. Mech. Design*, **104**, 307-313.